Atmospheric Pollution Research
www.atmospolres.com

Use of a process analysis tool for diagnostic study on fine particulate matter predictions in the U.S.–Part II: Analyses and sensitivity simulations

Ping Liu [1,2], Yang Zhang [2], Shaocai Yu [3], Kenneth L. Schere [3]

[1] *School of Environmental Science and Engineering, Shanghai Jiao Tong University, Shanghai, China*
[2] *Department of Marine, Earth, and Atmospheric Sciences, North Carolina State University, Raleigh, NC 27695*
[3] *Atmospheric Modeling and Analysis Division, the U.S. Environmental Protection Agency, Research Triangle Park, NC*

ABSTRACT

Following the Part I paper that describes an application of the U.S. EPA Models–3/Community Multiscale Air Quality (CMAQ) modeling system to the 1999 Southern Oxidants Study episode, this paper presents results from process analysis (PA) using the PA tool embedded in CMAQ and subsequent sensitivity simulations to estimate the impacts of major model uncertainties identified through PA. Aerosol processes and emissions are the most important production processes for $PM_{2.5}$ and its secondary components, while horizontal and vertical transport and dry deposition contribute to their removal. Cloud processes can contribute the production of $PM_{2.5}$ and SO_4^{2-} and the removal of NO_3^- and NH_4^+. The model biases between observed and simulated concentrations of $PM_{2.5}$ and its secondary inorganic components are found to correlate with aerosol processes and dry deposition at all sites from all networks and sometimes with emissions and cloud processes at some sites. Guided with PA results, specific uncertainties examined include the dry deposition of $PM_{2.5}$ species and its precursors, the emissions of $PM_{2.5}$ precursors, the cloud processes of SO_4^{2-}, and the gas–phase oxidation of SO_2. Adjusting the most influential processes/factors (i.e., emissions of NH_3 and SO_2, dry deposition velocity of HNO_3, and gas–phase oxidation of SO_2 by OH) is found to improve the model overall performance in terms of SO_4^{2-}, NO_3^-, and NH_4^+ predictions.

Keywords:
Fine Particulate Matter
CMAQ
Process Analysis
Sensitivity Study
1999 SOS

Article History:
Received: 18 March 2010
Revised: 17 August 2010
Accepted: 17 August 2010

Corresponding Author:
Yang Zhang
Tel: +1-919-5159688
Fax: +1-919-5157802
E-mail: yang_zhang@ncsu.edu

doi: 10.5094/APR.2011.008

1. Introduction

As described in Part I, three types of evaluation are performed: operational evaluation that calculates the statistics of observed and simulated concentrations of gaseous and PM species, diagnostic evaluation that analyzes dominant atmospheric processes and their contributions using the process analysis (PA) tool, and mechanistic evaluation (also referred to as sensitivity study) that examines the responses of the output variables to changes in the inputs and parameters for model treatments. Operational model evaluation for ozone (O_3) and fine particles ($PM_{2.5}$) simulated by regional air quality models such as the U.S. EPA Models–3/Community Multiscale Air Quality (CMAQ) modeling system (Binkowski and Roselle, 2003) using surface observations has been extensively performed (e.g., Yu et al., 2004; Arnold and Dennis, 2006; Zhang et al., 2006; Yu et al., 2008; Wu et al., 2008; Zhang et al., 2009a). Fewer studies, however, focus on diagnostic and process analysis (PA) that provide insights into the mechanism for their formation (e.g., Yu et al., 2008; Zhang et al., 2009b; Wang et al., 2009). Various probing tools have been developed to understand the roles of atmospheric processes in determining the fate of O_3 and $PM_{2.5}$ (Zhang et al., 2005). One such tool is the PA technique embedded in 3D air quality models, which calculates the Integrated Process Rates (IPRs) and Integrated Reaction Rates (IRRs). IPRs quantify the contributions of different physical and chemical processes to the concentrations of the species of interest; IRRs quantify the chemical evolution of gases. IRRs in CMAQ do not consider heterogeneous and aqueous reactions. However, the IRRs for the direct PM precursors such as HNO_3 and oxidants such as O_3 will help to understand the gas–phase chemistry that will affect PM formation. PA has been applied to study O_3 chemistry and transport (Jang et al., 1995; Jiang et al., 2003; O'Neill and Lamb, 2005; Tonse et al., 2008), the impacts of climate change on O_3 and particles (Hogrefe et al., 2005), particle number concentration and size distribution (Zhang et al., 2010b), and the dominant formation and removal process of $PM_{2.5}$ during different episodes (Yu et al., 2008; Wang et al., 2009).

Following an evaluation of CMAQ for its application to the 1999 Southern Oxidants Study episode described in Part I (Liu and Zhang, 2011), a detailed PA is conducted. Guided by PA, sensitivity simulations are designed to study the model responses to the uncertainties of major atmospheric processes and reactions identified by IPRs and IRRs analyses for inorganic $PM_{2.5}$. Our objective is to identify possible sources of model biases and improve model performance. Several areas of model improvement are identified in this work.

2. Methodology

The mass continuity equation in CMAQ is as follows:

$$\frac{\partial C_i}{\partial t} = -\left(u\frac{\partial C_i}{\partial x} + v\frac{\partial C_i}{\partial y} + w\frac{\partial C_i}{\partial z}\right) - \left[\frac{\partial}{\partial x}\left(K_x\frac{\partial C_i}{\partial x}\right) + \frac{\partial}{\partial y}\left(K_y\frac{\partial C_i}{\partial y}\right) + \frac{\partial}{\partial z}\left(K_z\frac{\partial C_i}{\partial z}\right)\right] + \left(\frac{\partial C_i}{\partial t}\right)_{emis} + \left(\frac{\partial C_i}{\partial t}\right)_{drydep} + \left(\frac{\partial C_i}{\partial t}\right)_{chem} + \left(\frac{\partial C_i}{\partial t}\right)_{aero} + \left(\frac{\partial C_i}{\partial t}\right)_{cloud} \quad (1)$$

where $\partial C_i/\partial t$ is the change of concentration of species *i* with time; the first term on the right–hand side of Equation (1) is the advection in the *x*, *y*, and *z* directions, and *u*, *v*, and *w* are the wind velocity components in the three directions; the second term is the diffusion term and K_x, K_y, and K_z are turbulent diffusivities; the remaining five terms are the rates of change of species concentration due to emissions, dry deposition, gas–phase chemical reactions, aerosol processes, and cloud processes, respectively. IPRs compute the rates of change of species concentration due to horizontal transport, vertical transport, emissions, dry deposition, gas–phase chemistry, aerosol processes, cloud processes, and mass balance adjustment. Horizontal transport is the sum of horizontal advection and diffusion. Vertical transport is the sum of vertical advection and diffusion. Aerosol processes represent the net effect of aerosol thermodynamics, gas–to–particle mass transfer [e.g., homogeneous nucleation and condensation of sulfuric acid and organic carbon (OC) on preexisting particles], and coagulation within and between Aitken and accumulation modes. Cloud processes represent the net effect of cloud attenuation of photolytic rates, aqueous–phase chemistry, below– and in–cloud mixing, cloud scavenging, and wet deposition. The mass balance adjustment is used to compensate for the mass inconsistency of species. IRRs calculate the rates of change of species concentration due to 214 individual reactions for 72 species simulated in the Statewide Air Pollution Research Center Mechanism (SAPRC99) (Carter, 2000) in CMAQ. The IRRs of 214 reactions are grouped into 34 products according to the reactions for radical initiation, propagation, production, and termination. They are listed in Table S1 in the Supporting Material (SM). The IPRs and IRRs are calculated and analyzed for mass of $PM_{2.5}$ and its species, and gaseous precursors of secondary $PM_{2.5}$. The correlation between different processes and large model biases of PM species is analyzed to identify the most influential processes [i.e., those having the strongest correlation (with correlation coefficients of 0.45 or greater) with the model biases]. The chemical regimes of O_3 chemistry [i.e., nitrogen oxides (NO_X = NO + NO_2) or volatile organic compounds (VOCs) – limited conditions] and chemistry of major gas–phase oxidants and $PM_{2.5}$ precursors are examined through IRRs analyses. Eight sites from the Southeastern Aerosol Research and Characterization (SEARCH) are selected to contrast surface and column IPRs analyses. These include four urban sites [i.e., Jefferson Street in Atlanta (JST), GA; North Birmingham (BHM), AL; Gulfport (GFP), MS; Pensacola (PNS), FL], three rural sites [i.e., Yorkville (YRK), GA; Centreville (CTR), AL; Oak Grove (OAK), MS], and one suburban site [i.e., Outlying field (OLF), FL] (see site locations in Figure S1 in the SM).

Subsequent sensitivity simulations that are designed based on process analysis results presented in Sections 3.1 and 3.2. These simulations are conducted to characterize the model responses to the uncertainties of major production and removal processes and reactions identified by IPRs and IRRs analyses for inorganic $PM_{2.5}$. The sensitivity simulations include simulations using adjusted dry deposition velocities of $PM_{2.5}$ species and its precursors, adjusted emissions of $PM_{2.5}$ precursors, and adjusted parameters involved in the cloud processes of SO_4^{2-}, and the gas–phase oxidation of SO_2. The rationales for these sensitivity simulations along with the results are described in more detailed in Section 3.3.

3. Results and Discussions

3.1. IRRs analyses

Figure 1a shows the spatial distribution of the 15–day mean chemical production of total odd oxygen (O_X). O_X is the sum of O_3, ground state oxygen atom (O), exited oxygen atom [$O^1(D)$], nitrogen dioxide (NO_2), peroxynitric acid (HNO_4), nitric acid (HNO_3), nitrate radical (NO_3), and dinitrogen pentoxide (N_2O_5) [i.e., O_X = O_3 + O + $O^1(D)$ + NO_2 + HNO_4 + HNO_3 + $2NO_3$ + $3N_2O_5$]. The total O_X production is significant (at a rate of > 3 ppb hr^{-1}) in the eastern U.S. and California where high O_3 episodes usually occur. Two photochemical indicators are used to determine the VOC– or NO_X–sensitive regimes: afternoon reactive nitrogen [NO_y = NO_X+ nitrogen trioxide (NO_3) + dinitrogen pentoxide (N_2O_5) + nitrous acid (HONO) + nitric acid (HNO_3) + pernitric acid (HNO_4) + peroxyacyl nitrate (PAN)] recommended by Sillman (1995) and the ratio of production rates of peroxides (H_2O_2) and HNO_3 (P_{H2O2}/P_{HNO3}) proposed by Tonnesen and Dennis (2000). The afternoon NO_y mixing ratio larger than 20 ppb indicates a VOC–sensitive chemistry (Sillman, 1995). The value of P_{H2O2}/P_{HNO3} less than 0.06 at any time during the day indicates a VOC–sensitive chemistry (Tonnesen and Dennis, 2000).

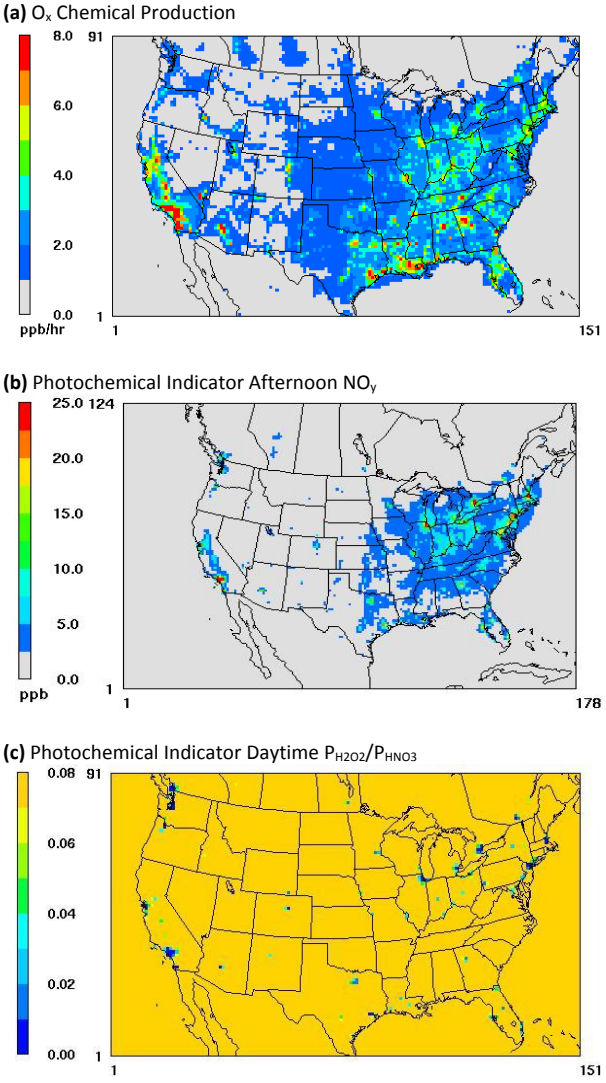

Figure 1. *Spatial distributions of 15-day mean of* ***(a)*** *total O_x chemical production rate and photochemical indicator of* ***(b)*** *NO_y (ppb) during afternoon (1:00-5:00 pm) and* ***(c)*** *P_{H2O2}/P_{HNO3} during daytime predicted by CMAQ during June 14-28, 1999.*

The photochemical indicators calculated based on observations are subject to some uncertainties. These include uncertain dry/wet deposition rates, aerosol processes, measurement errors, mechanism dependence, and case–to–case variations (Sillman and He, 2002). As shown in Figures 1b and 1c, a few cities over the west coast of California, New England area, the Great Lakes, and Ohio valley in the mid–west are primarily dominated by VOC–sensitive chemistry. This is indicated by occurrences of NO_y > 20 ppb and P_{H2O2}/P_{HNO3} < 0.06 over these regions. This is due to the relatively higher NO_X emissions in those urban areas. Some regions (e.g., Phoenix, Houston, Dallas, and the Colorado Front range) have P_{H2O2}/P_{HNO3} < 0.06 but NO_y < 20 ppb. This may indicate a slight dominance of VOC–sensitive chemistry or a chemistry that may be sensitive to both VOC and NO_X emissions (the so–called ridge line). By contrast, most rural and remote areas, where VOC emissions are high, are primarily dominated by NO_X–sensitive chemistry. The ratio of P_{H2O2}/P_{HNO3} identifies slightly larger areas with VOC–sensitive chemistry than NO_y, likely because the indicator involving H_2O_2 appears to be more robust (Tonnesen and Dennis, 2000). Figure 2 shows the amounts of hydroxyl radical (OH) consumed by anthropogenic and biogenic VOCs (AVOCs and BVOCs) to produce O_3. OH radicals reacted with BVOCs are greater than 0.75 ppb hr^{-1} in the southeastern U.S. and California, with a maximum of 2.5 ppb hr^{-1} occurred in California. OH radicals reacted with AVOCs are high in the mid–west, Texas, and the west coast in California, with a maximum of 3.2 ppb hr^{-1} occurred in California. The dominance of VOC emissions and their subsequent oxidations by OH over most U.S. areas lead to a NO_X–limited O_3 chemistry in those regions.

In SAPRC99, HNO_3, a precursor of NO_3^-, is formed or depleted via three major pathways:

$$OH + NO_2 \rightarrow HNO_3 \quad (2)$$

$$HC + NO_3 \rightarrow HNO_3 \quad (3)$$

$$OH + HNO_3 \rightarrow NO_3 \quad (4)$$

where HC represents non–methane hydrocarbons. Figure S2 (see the SM) shows the daily totals of P_{HNO3} from Reactions (2) and (3) and the depletion of HNO_3 from Reaction (4) at an urban (JST) and a rural site (YRK) in Georgia. On average, 95–98% of the production of HNO_3 can be attributed to Reaction (2). OH can only consume < 1% of total HNO_3 to produce NO_3. This indicates other dominant pathways such as dry and wet deposition may contribute mostly to the removal of HNO_3 at both sites.

3.2. IPRs analysis

Column and export analysis. The IPRs are calculated as an average of hourly values for a column block of horizontal grid cells in the planetary boundary layer (PBL, defined to be the first 14 layers of the 21 layers used in CMAQ simulation, corresponding to 0–2.6 km above the ground level) at each site for the 15–day period. The block is defined as the grid cell in which the site is located and its eight surrounding grid cells. This is because one grid cell cannot be viewed independently, and the horizontal transport from the adjacent grid cells can play an important role in the variations of pollutant concentrations. The net domainwide average exports of air pollutants are calculated as the sum of process contributions of emissions, gas–phase chemistry, aerosol processes, cloud processes, and dry deposition in the PBL. The positive values indicate export out of the PBL into the free troposphere (using free troposphere as a reference box for fluxes in or out). The negative values indicate import from the free troposphere into the PBL. Eight SEARCH sites are selected for IPR analysis, and they are grouped as urban (i.e., JST, BHM, GFP, and PNS) and rural/suburban sites (i.e., YRK, CTR, OAK, and OLF).

Figure 3 shows the process contributions of $PM_{2.5}$, sulfate (SO_4^{2-}), nitrate (NO_3^-), ammonium (NH_4^+), and their precursors, sulfur dioxide (SO_2), HNO_3, ammonia (NH_3), and NO_X at the SEARCH sites. The contributions of processes (except for emissions) of $PM_{2.5}$ are similar to those of SO_4^{2-} for two reasons. First, the SO_4^{2-} concentrations dominate in $PM_{2.5}$ mass concentrations (by > 49%) at both urban and rural sites. Second, the major sources of $PM_{2.5}$ emissions are elemental carbon (EC) and primary OC. The contributions of dry deposition to the removal of all species except for HNO_3 are relatively small. In both urban and rural areas, horizontal and vertical transports, dry deposition, and wet depositions remove the pollutants from the column and contribute to the loss of $PM_{2.5}$ and SO_4^{2-}. Aerosol processes such as homogenous nucleation and condensation, cloud processes such as aqueous–phase chemistry, and emissions contribute to their production. Unlike $PM_{2.5}$ and SO_4^{2-}, horizontal transport contributes to the increase of NO_3^- in the rural area. The opposite role of horizontal transport in different PM species may occur under some circumstances. For example, when winds pass an upwind location where the air is rich in NO_3^- but poor in SO_4^{2-}, it would add NO_3^- to the existing NO_3^- concentration (positive) at a receptor, but it would dilute the existing SO_4^{2-} concentration (negative) at the same receptor. When the dilution effect dominates over the addition effect, $PM_{2.5}$ concentrations will also decrease due to a dominance of SO_4^{2-} concentrations in $PM_{2.5}$ concentrations. Aerosol processes contribute to the increase of NO_3^- in both areas. Cloud processes contribute to the removal of NO_3^- and NH_4^+ in both areas. This is mainly due to the dominance of the in–cloud equilibrium chemistry, cloud mixing and scavenging, and subsequent wet deposition. Note that this is different from the effect of cloud processes on sulfate, for which sulfate concentrations are increased due to the dominance of in–cloud SO_4^{2-} production over other cloud processes. Vertical transport contributes to the removal NO_3^- and NH_4^+ in both areas, indicating that the air mass with high NO_3^- and NH_4^+ may have been transferred into the column block above the stations. Dry deposition contributes to the removal of all species.

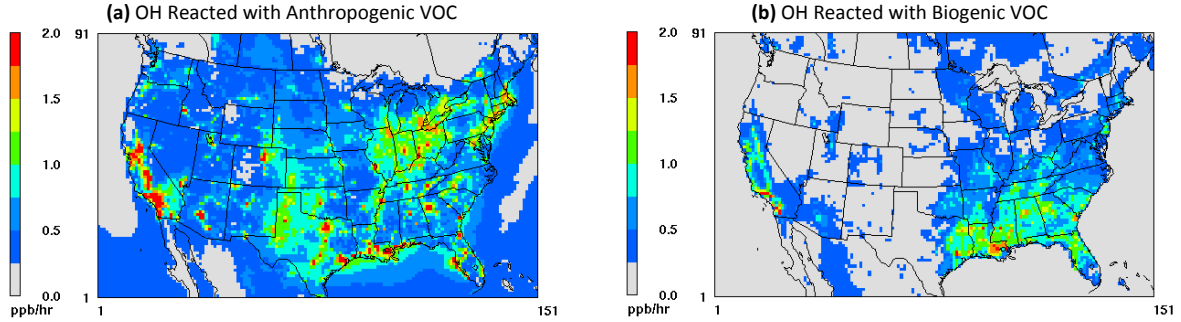

Figure 2. *Spatial distributions of 15-day mean of* ***(a)*** *OH reacted with anthropogenic VOCs, and* ***(b)*** *OH reacted with biogenic VOCs predicted by CMAQ during June 14-28, 1999.*

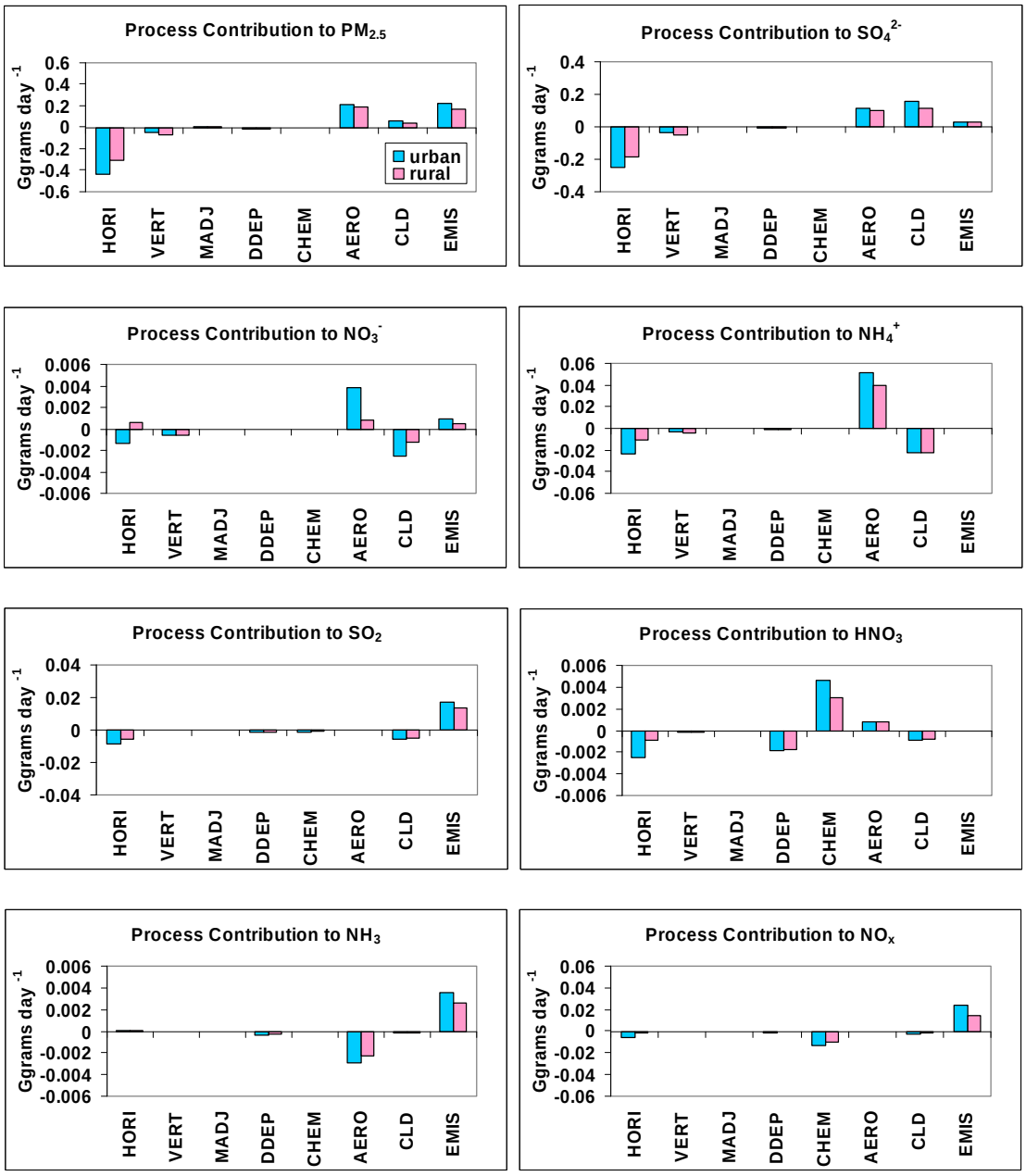

Figure 3. *Contributions (Ggrams day^{-1}) of horizontal transport (HORI), vertical transport (VERT), mass balance adjustment (MADJ), dry deposition (DDEP), gas-phase chemistry (CHEM), aerosol processes (AERO), cloud processes (CLD), and emissions (EMIS) to the concentration change of $PM_{2.5}$, SO_4^{2-}, NO_3^-, NH_4^+, SO_2, HNO_3, NH_3, and NO_X predicted by CMAQ at the SEARCH sites during June 14-28, 1999.*

Emissions are important sources for PM precursors, including SO_2, NO_X, and NH_3. Dry deposition is an important removal process for all PM precursors, particularly for HNO_3. Gas–phase chemistry depletes SO_2 and NO_X through their oxidation by OH radicals, but increases the level of HNO_3 via Reactions (2) and (3). Aerosol processes contribute to a decrease in NH_3 but an increase in HNO_3. The increase in NO_3^- is slightly greater than that in HNO_3 in urban areas, indicating that the gas–particle equilibrium favors the formation of NO_3^-. The increase in HNO_3 is slightly greater than that in NO_3^- in rural areas, indicating that the gas–particle equilibrium favors the volatility of NO_3^- to the gas–phase to form HNO_3. Cloud processes remove all these gases, with a large removal rate for SO_2 and HNO_3 than NH_3 and NO_X. Most processes will be further examined in the correlation analysis in the next section.

Table 1 summarizes the 15–day average of net domainwide process contributions and exports of O_X, O_3, NO_X, NO_Y, HNO_3, SO_2, AVOC, BVOC, and $PM_{2.5}$ from the PBL to free troposphere. Relatively large amounts of O_X, O_3, AVOCs, and $PM_{2.5}$ can be exported from the PBL to the free troposphere. Such exports of pollutants enhance the total oxidation capacity in the middle and upper troposphere. They can thus affect the concentrations of pollutants at surface or in the PBL and modulate the local meteorology/climate in other regions. For example, the secondary pollutants in the upper troposphere can transport to the ground through vertical mixing. Aerosol feedbacks [e.g., direct effects via radiation reduction and indirect effects via serving as cloud condensation nuclei (CCN)] to PBL meteorology can affect temperature (T), relative humidity (RH), and wind (Zhang, 2008; Zhang et al., 2010a) (though such feedbacks are not treated in CMAQ used here).

IPRs Correlation analysis. The relationship between model biases and major atmospheric processes may provide guidance for sensitivity studies. To further understand such a relationship, the correlation of the large model errors and the contributions of individual processes are analyzed for $PM_{2.5}$, SO_4^{2-}, NO_3^-, and NH_4^+

Table 1. *The net domainwide export of O_x, O_3, NO_x, NO_y, HNO_3, SO_2, AVOC, BVOC, and $PM_{2.5}$ from the planetary boundary layer (PBL) to the free troposphere during June 14-28, 1999, the unit is G mole/day for gas species and G gram/day for PM species*

Process	O_x	O_3	NO_x	NO_y	HNO_3	SO_2	AVOC	BVOC	$PM_{2.5}$
Dry deposition	-5.21	-4.70	-0.11	-0.54	-0.35	-0.15	-0.97	0.00	-2.02
Gas-phase chemistry	6.39	5.18	-1.16	-0.17	0.50	-0.13	-2.20	-9.69	0.00
Aerosol processes	-0.06	0.00	0.00	-0.01	0.12	0.00	0.00	0.00	20.50
Cloud processes	0.25	0.55	-0.09	-0.30	-0.15	-0.36	-1.12	-0.34	-10.30
Emissions	0.06	0.00	1.43	1.43	0.00	0.72	6.86	10.65	12.01
Net export	1.44	1.03	0.07	0.42	0.12	0.08	2.57	0.61	20.19

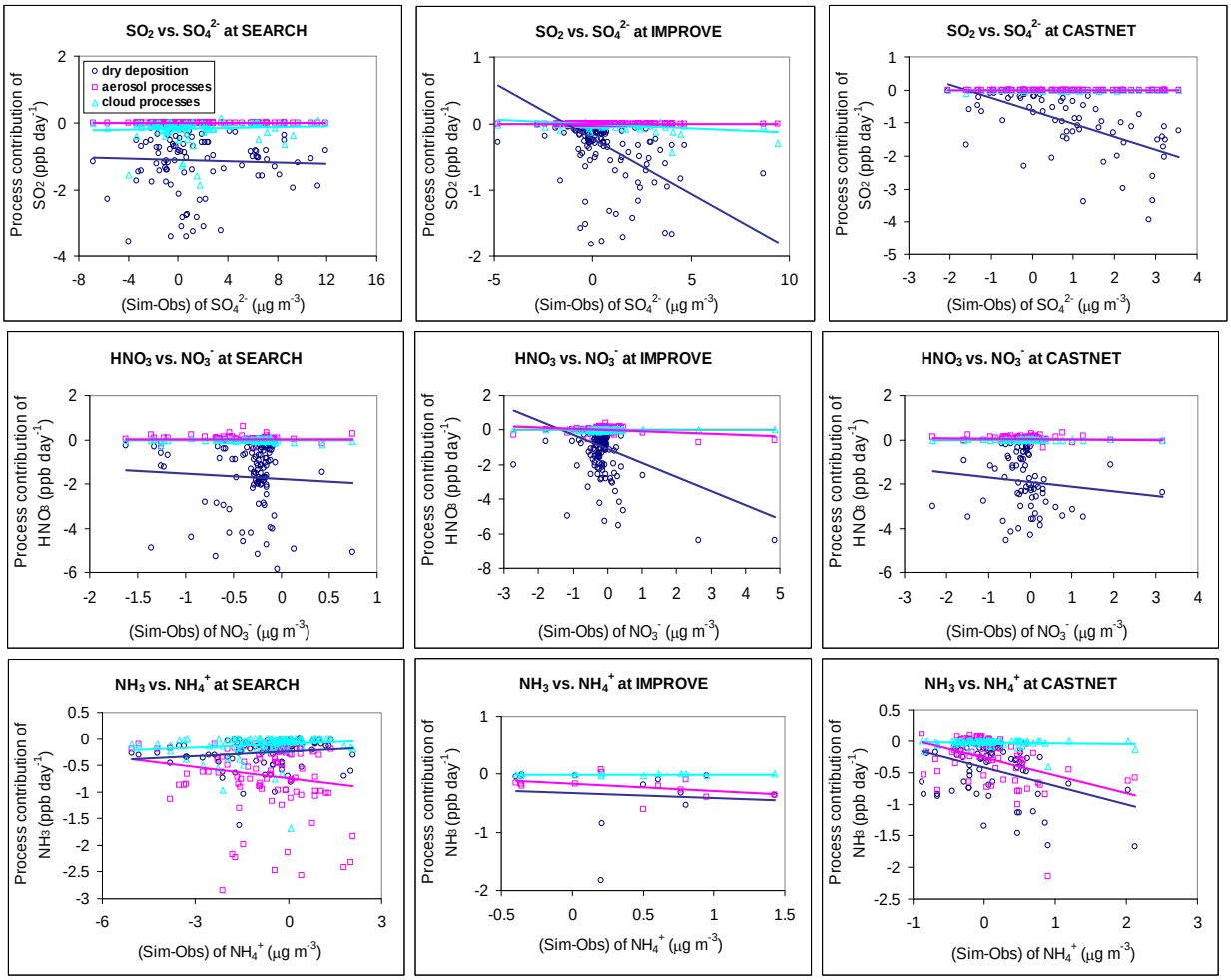

Figure 4. *Scatter plots of contributions of aerosol processes (pink square), cloud processes (blue triangle), and dry deposition (black circle) of PM precursors (i.e., SO_2, HNO_3, and NH_3) versus large model biases for corresponding PM (i.e., SO_4^{2-}, NO_3^-, and NH_4^+) (by CMAQ), respectively, at the SEARCH, IMPROVE, and CASTNET sites during June 14-28, 1999.*

at the SEARCH, the Clean Air Status and Trends Network (CASTNET), the Interagency Monitoring of Protected Visual Environments (IMPROVE), and the Speciation Trends Network (STN) sites. The large model error here is defined as the absolute difference between predictions and observations that is greater than 20%. It is assumed that if a particular process is highly correlated with the large errors, and this process is likely to contribute to the model biases and will be examined further through sensitivity simulations.

Correlations of emission contributions of major $PM_{2.5}$ precursors (i.e., SO_2, NO_X, and NH_3) with PM biases are shown in Figure S3 (see the SM). The corresponding correlation coefficients are summarized in Table 2. SO_2 emissions are correlated with SO_4^{2-} biases at the SEARCH, IMPROVE, and CASTNET sites except for a few outliers. NH_3 emissions are correlated with NH_4^+ biases at the CASTNET sites. NO_X emissions are correlated with NO_3^- biases at the IMPROVE and CASTNET sites except for a few outliers. They are slightly negatively correlated at the SEARCH sites, especially at the urban sites. As shown in Figure 4, there are no obvious correlations found between PM biases and cloud processes of all three $PM_{2.5}$ precursors (i.e., SO_2, HNO_3, and NH_3) or aerosol processes of SO_2 and HNO_3. Dry deposition of SO_2 and HNO_3 are negatively–correlated with the model biases for SO_4^{2-} and NO_3^-, respectively, at the IMPROVE and CASTNET sites. Dry deposition of NH_3 is negatively–correlated with the NH_4^+ biases at the CASTNET sites (i.e., largely at rural sites), but slightly correlated at the SEARCH sites.

Aerosol processes of NH_3 are negatively–correlated with NH_4^+ biases at both the SEARCH and CASTNET sites. This indicates the conversion of NH_3 to ammonium nitrate (NH_4NO_3). Moreover,

aerosol processes may not be the major contributors to NH_4^+ overpredictions at the CASTNET and IMPROVE sites. NH_3 emissions are the largest contributors to the NH_4^+ biases (see Figure S3 in the SM and Table 2), especially at the CASTNET sites with a correlation coefficient (R) of 0.46.

Figure 5 shows the correlation between different processes and large model biases for $PM_{2.5}$, SO_4^{2-}, NO_3^-, and NH_4^+ for various networks. Similar plots at the SEARCH sites accounting for all, urban or rural sites separately are also provided in Figure S4 (see the SM). The R values between various processes and model biases for these species at all sites from various networks are given in Table 2. Among all processes studied, the following six processes have large R values (≥ 0.45) with one or more PM species. These processes are considered to be most influential processes. Horizontal transport is highly correlated with $PM_{2.5}$ biases at the STN sites (R = 0.72). Vertical transport is correlated with SO_4^{2-} biases with R values of 0.45–0.47 at rural sites from SEARCH and IMPROVE. Dry deposition is negatively–correlated with biases of $PM_{2.5}$ and its inorganic components at all urban and rural sites (except for NO_3^- at the rural sites) with R values of –0.7 to –0.2. Higher dry deposition flux in terms of absolute values (ignoring the negative sign, which indicates a removal process) corresponds to higher simulated concentrations (i.e., the model overpredictions). This is because the deposition flux is proportional to the species concentration and deposition velocity. Aerosol processes are negatively–correlated with $PM_{2.5}$ biases at the STN sites (with R = –0.7). It is, however, positively correlated with SO_4^{2-} biases (with R from 0.5 to 0.6) at the SEARCH rural sites and the CASTNET sites. Note that opposite correlations exist between aerosol processes and $PM_{2.5}$ biases at STN vs. other networks and between aerosol processes and biases of NH_4^+ and NO_3^- at the SEARCH urban vs. rural sites under dry conditions or NH_3–rich conditions (see Figures S5 and S6 in the SM) when large model biases occur in the PM model treatments (e.g., the inorganic thermodynamic equilibrium in ISORROPIA). Cloud processes are correlated with model biases for NH_4^+ at the SEARCH rural sites (with R = 0.5) but negatively–correlated with NO_3^- at the CASTNET sites (R = –0.5). Among three major PM precursors, emissions of NH_3 correlate with NH_4^+ at the CATSNET sites (R = –0.45).

3.3. Sensitivity simulations

The above PA results show that emissions (e.g., NH_3 emissions), aerosol/cloud processes, and dry deposition of PM precursors may contribute to the model biases of the secondary PM. With the guidance from PA, sensitivity simulations for those processes are subsequently conducted to analyze the model responses to NO_X– vs. VOC–limited regimes identified via IRRs, as well as changes in key processes and reactions identified via IPRs, aiming to reduce model biases. While horizontal and vertical transport processes also show a large correlation with PM species, the perturbation of parameters related to those processes only will cause self–inconsistency among meteorological variables. The sensitivity simulations regarding these meteorological processes are therefore not considered in this study.

NO_X– vs. VOC–sensitivity of O_3 chemistry. Using P_{H2O2}/P_{HNO3} as a photochemical indicator, O_3 formation over most U.S. is dominated by NO_X–sensitive chemistry, and that in California, New England, and the Great Lakes and Ohio valley in the mid–west are primarily dominated by VOC–sensitive chemistry (Section 3.1). Two sensitivity simulations are conducted with 50% domainwide reduction of NO_X and VOC emissions. These simulations simulate the responses of O_3 mixing ratios to changes in its precursor emissions and verify whether the indicators are robust to distinguish the two regimes. As shown in Figure 6, reducing 50% the VOC emissions results in lower O_3 mixing ratios (mostly by 2–6 ppb, or by 4–8%) in California and the Great Lakes and Ohio valley in the mid–west, compared with baseline results. Reducing 50% NO_X emissions results in lower O_3 mixing ratios (mostly by 2–15 ppb, or by 4–20%) in most U.S., indicating a dominance of the NO_X–sensitive O_3 chemistry over most U.S. These results are consistent with results based on P_{H2O2}/P_{HNO3} described in Section 3.1. However, increasing the O_3 mixing ratios occur with 50% NO_X emission reduction at some locations in California, mid–western, north eastern, and southern U.S., due either a VOC–limited O_3 chemistry or an accumulation of O_3 dominated by transport, or both over those areas. Such O_3 disbenefits from NO_X emission control are also reported by Arnold and Dennis (2006) at JST using SAPRC99 and by Zhang et al. (2009b) using the carbon bond (CB–IV) gas–phase mechanism.

Table 2. *Correlation coefficient (R) of different processes and model biases in various species concentrations simulated by CMAQ[a, b]*

Processes	SEARCH								IMPROVE				CASTNET			STN
	Urban Sites				Rural Sites											
	$PM_{2.5}$	SO_4^{2-}	NO_3^-	NH_4^+	$PM_{2.5}$	SO_4^{2-}	NO_3^-	NH_4^+	$PM_{2.5}$	SO_4^{2-}	NO_3^-	NH_4^+	SO_4^{2-}	NO_3^-	NH_4^+	$PM_{2.5}$
Horizontal Transport	-0.42	-0.30	-0.19	-0.29	0.05	-0.24	-0.20	-0.08	-0.20	-0.06	-0.34	-0.24	-0.19	-0.06	-0.30	**0.72**
Vertical Transport	-0.36	0.28	0.29	-0.29	-0.01	**0.45**	-0.10	0.10	-0.12	**0.47**	-0.41	-0.22	0.42	-0.17	-0.39	-0.04
Emissions	0.40	0.25	-0.08	--	0.01	-0.10	0.06	--	0.15	0.11	0.27	--	0.25	0.18	--	-0.07
Dry Deposition	**-0.53**	**-0.58**	-0.34	-0.40	**-0.64**	**-0.71**	0.05	-0.21	-0.20	**-0.66**	**-0.72**	-0.31	**-0.61**	**-0.62**	-0.42	-0.23
Aerosol Processes	0.35	0.12	-0.17	0.30	0.20	**0.47**	0.10	-0.18	0.17	0.35	0.40	0.40	**0.60**	0.25	0.42	**-0.72**
Clouds Processes	-0.04	-0.03	-0.04	-0.05	0.30	0.12	-0.01	**0.47**	-0.04	-0.27	-0.06	0.16	-0.04	**-0.51**	-0.04	-0.24
SO_2 Emissions[c]	----	0.24	----	----	----	-0.13	----	----	----	0.16	----	----	0.15	----	----	----
NO_x Emissions[c]	----	----	-0.05	----	----	----	-0.01	----	----	----	0.33	----	----	0.34	----	----
NH_3 Emissions[c]	----	----	----	0.20	----	----	----	-0.39	----	----	----	0.43	----	----	**0.46**	----

[a] *"--" indicates no direct process contributions for direct emissions. For example, NH_4^+ is a secondary pollutant and has no emissions. Emissions refer to emissions of all listed species, e.g., emissions of EC and primary OM, SO_4^{2-}, and NO_3^- for $PM_{2.5}$, primary SO_4^{2-} emissions for SO_4^{2-} and primary NO_3^- emissions for NO_3^-.*

[b] *The values in bold indicate large correlation coefficients.*

[c] *For emissions of SO_2, NO_x, and NH_3, R values were calculated only for the directly relevant species (e.g., SO_2 emissions will directly affect SO_4^{2-}), although other species may also be affected (e.g., SO_2 emissions will affect the formation of NH_4^+, NO_3^-, and $PM_{2.5}$). Those R values correspond to correlation plots in Figures A-2. R values for other species that are not calculated are indicated with by "----".*

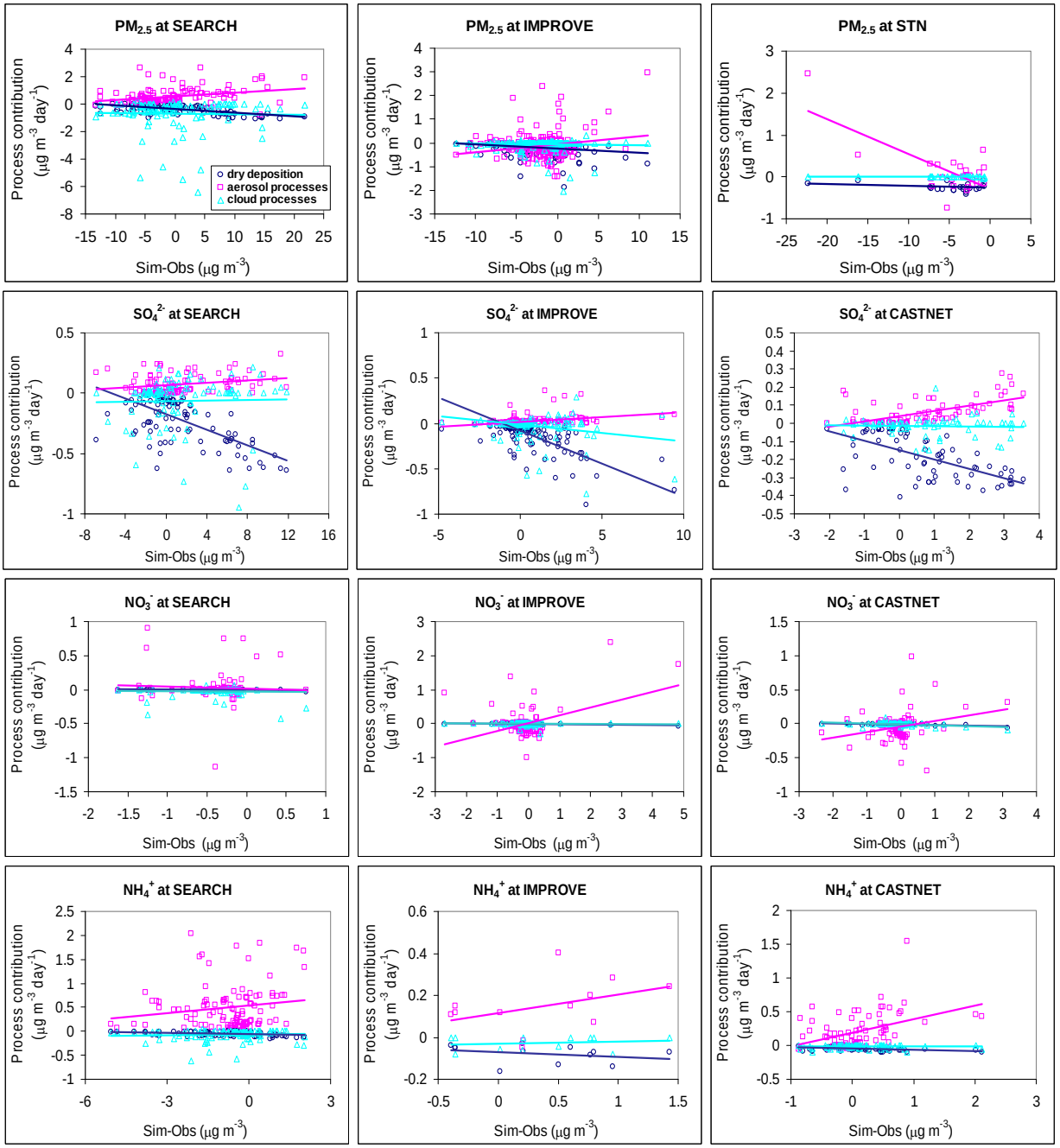

Figure 5. *Scatter plots of process contributions of aerosol processes (pink square), cloud processes (blue triangle), and dry deposition (black circle) versus large model biases for $PM_{2.5}$, SO_4^{2-}, NO_3^-, and NH_4^+ (by CMAQ) at the SEARCH, IMPROVE, CASTNET, and STN sites during June 14-28, 1999. Observed $PM_{2.5}$ is not available at the CASTNET sites, and observed PM components are not available at the STN sites for this episode.*

Emissions of $PM_{2.5}$ precursors. The emissions used in this study are based on the U.S. EPA's 1999 National Emission Inventory (NEI) v.3. The total emissions of NH_3, an important precursor of NH_4^+, is compared with the results from the Carnegie Mellon University (CMU) national NH_3 emission inventory (http://www.cmu.edu/ammonia/) (Goebes et al., 2003) that is considered to be more accurate than the NEI v.3 for several reasons (Wu et al., 2008). For example, the CMU NH_3 inventory provides the process–based and temporally- and spatially-resolved estimates for fertilizer and dairy cattle. The dependence of NH_3 emissions on climate conditions, farming practice, and the geographic variation of animal population is taken into account in the CMU inventory. Compared with the CMU NH_3 inventory, NEI v.3 used here gives NH_3 emissions that are lowered by 25.5% on average domainwide for this episode. A factor of 1.2551 is therefore applied to adjust total NH_3 emission uniformly for the entire domain in the sensitivity simulation.

As shown in Figure 7, the sensitivity simulation results show that increased NH_3 emissions can cause increased NO_3^- and NH_4^+ since more NH_3 is available to form NH_4NO_3. Increasing NH_3 emissions can increase NO_3^- by 43–73%. The NMBs of NO_3^- change from –45%, –75%, and –22% of the baseline simulation to –23%, –56%, and 14% of the sensitivity simulation at the IMPROVE, SEARCH, and CASTNET sites, respectively. The NMB of NH_4^+ changes from –32% to –20% at the SEARCH sites, but from 24% to 42% at the IMPROVE sites and from 8% to 22% at the CASTNET sites (i.e., a worse performance) since NH_4^+ is already over-predicted by the baseline simulation at these two sites. Those results indicate that increasing NH_3 emissions can significantly improve model performance of NO_3^- and NH_4^+ when they are underpredicted. Under such conditions, NO_3^- formation depends on the availability of NH_3. There are no significant impacts on SO_4^{2-} and $PM_{2.5}$. This is likely due to the sulfate–poor (i.e., NH_3–rich; $[NH_4^+]/[SO_4^{2-}] > 2$) condition at those sites (e.g., observed and

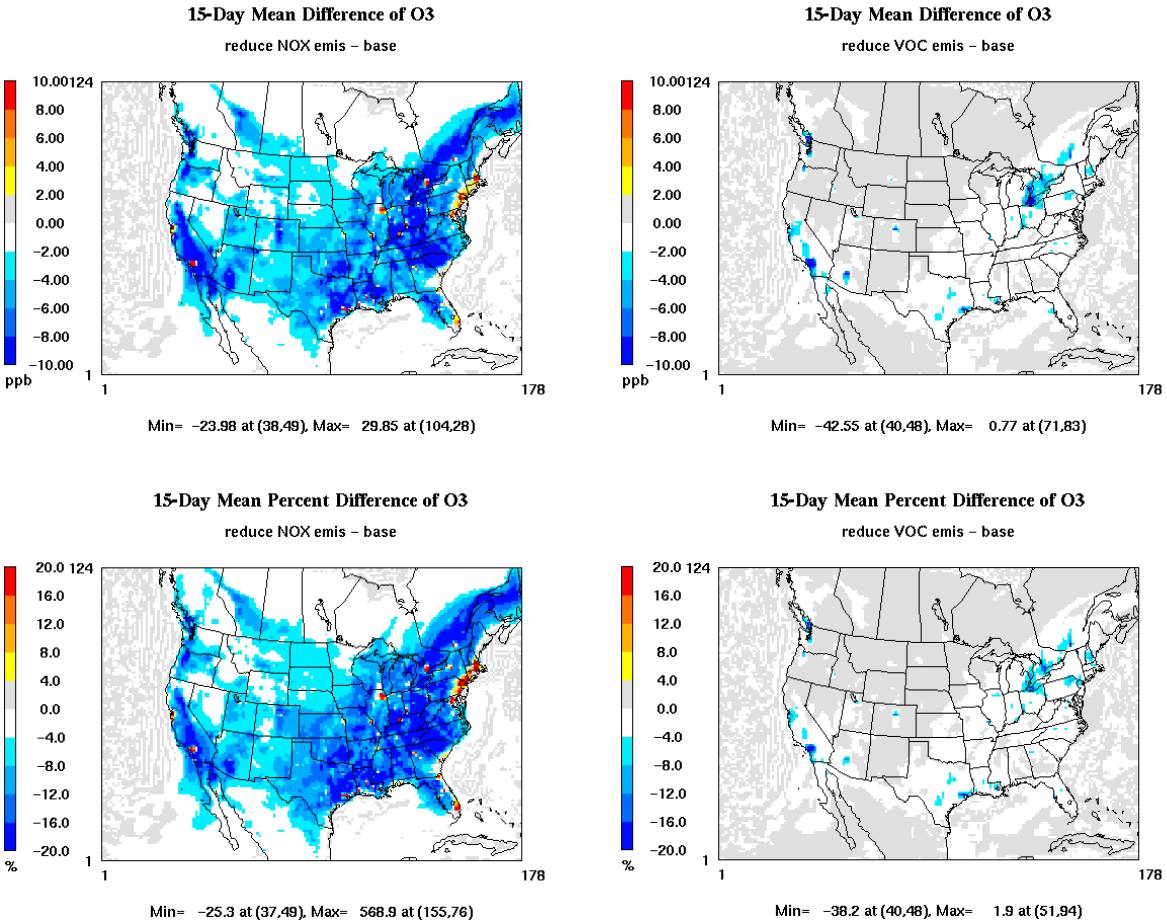

Figure 6. *The absolute and percentage difference of hourly O_3 between the CMAQ simulations with 50% reduction of NO_X and VOC emissions and the baseline simulation in June 14-28, 1999.*

simulated average $[NH_4^+]/[SO_4^{2-}]$ is greater than 4 at the IMPROVE sites). SO_4^{2-} is neutralized by NH_3, and the increased NH_3 is able to neutralize more NO_3^-. To explore the effect of scaling emissions of SO_2 on SO_4^{2-} and other inorganic aerosol concentrations, a sensitivity simulation with 20% reduced SO_2 emissions is also conducted based on the NMBs of 18–20% in the baseline predictions of SO_4^{2-}. Reducing SO_2 emissions by 20% can reduce SO_4^{2-} by 15–16% and reduce the NMBs from 20% to 3%, 24% to 5%, and 18% to 1% at the IMPROVE, SEARCH, and CASTNET sites. Decreasing SO_4^{2-} makes more NH_3 available to form NH_4NO_3. This will increase NO_3^- concentration but decrease NH_4^+ concentration due to the replacement of ammonium sulfate $[(NH_4)_2SO_4]$ by NH_4NO_3. Such a replacement requires more NH_4^+ to evaporate back to the gas–phase to maintain the ionic balance, thus increasing NH_4^+ underpredictions as compared to the baseline simulation.

3.4. Dry Deposition

$PM_{2.5}$ species. Dry deposition is an important removal process for $PM_{2.5}$ species as shown in the previous IPRs analyses. Two methods are used to investigate the effects of dry deposition on major $PM_{2.5}$ species, especially SO_4^{2-}: directly adjusting dry deposition velocity of SO_4^{2-} and adjusting dry deposition flux of the accumulation mode with most fine SO_4^{2-}. A 20% increase of SO_4^{2-} dry deposition velocity or fluxes is applied in the above methods based on ~20% overprediction of SO_4^{2-} in the baseline simulation. The impacts of these two adjustments are negligible for PM species simulations. For example, at the IMPROVE and CASTNET sites, the NMBs of SO_4^{2-} are improved from 20% to 19% and from 18% to 17%. One possible reason is that the overprediction of SO_4^{2-} concentration is so significant that makes the impact of increased dry deposition fluxes negligible, since the latter is proportional to the species concentration and deposition velocity. The impact of adjustment of deposition velocity is small relative to the concentration variations. Although the relations of deposition of PM species are identified in the IPR correlation analysis, there is no significant evidence showing in sensitivity simulations due to the nearly negligible magnitudes of the contributions from the deposition of PM species to model biases.

$PM_{2.5}$ precursors. Dry deposition is a major removal process for $PM_{2.5}$ precursors (e.g., HNO_3, SO_2, and NH_3). Three sensitivity simulations are set up to test the model responses to the dry deposition velocities of those precursors. The typical dry deposition velocities, V_d, are 4 cm s^{-1} over land for HNO_3 (Seinfeld and Pandis, 2006), 0.8–1.2 cm s^{-1} in June for SO_2 (Finkelstein et al., 2000), and 3.94 ± 2.79 cm s^{-1} during the day and 0.76 ± 1.69 cm s^{-1} during nighttime in summer at North Carolina (Phillips et al., 2004). Based on these values reported in the literature and the differences between V_d values used in CMAQ, the simulated V_d values of HNO_3, SO_2, and NH_3 are adjusted by a factor of 0.5, 1.2, and 0.5, respectively, uniformly for the entire domain.

As shown in Figures 7d–6f, with a 50% reduction in the V_d of HNO_3, the NMBs of NO_3^- reduce from –45% to –29%, –75% to –69%, and –22% to –1% at the IMPROVE, SEARCH, and CASTNET sites, respectively, despite no significant change in the model performance for NH_4^+, SO_4^{2-}, and $PM_{2.5}$. Compared with results from the baseline simulation, the sensitivity simulation with a reduced V_d of HNO_3 gives higher HNO_3 (by 38% on average). This in turn increases NO_3^- by 27%, 29%, and 22% for the three networks,

respectively. The predictions for NH_4^+, SO_4^{2-}, and $PM_{2.5}$ generally remain the same as the baseline values. This is because NO_3^- constitutes a small fraction of total $PM_{2.5}$ (i.e., about 3%) at the IMPROVE and SEARCH sites. Reduction of the V_d of NH_3 by 50% can increase NO_3^- by 18–21% and reduce the NMBs of NO_3^- from 45% to 35%, 75% to 70%, and 22% to 8% at the IMPROVE, SEARCH, and CASTNET sites, respectively. However, the NMB of NH_4^+ increases from 24% to 31% at the IMPROVE sites. Similar effects can be found at the SEARCH and CASTNET sites but with small magnitudes. Under conditions with sufficient NO_X and low sulfate (e.g., sulfate–poor conditions), increased NH_3 can cause increased NH_4^+ and NO_3^-. This is because more NH_4NO_3 can be formed following the formation of $(NH_4)_2SO_4$. Sulfate decreases about 2% and the sensitivity simulation reduces the NMBs from 20% to 17%, 24% to 21%, and 18% to 15% at the IMPROVE, SEARCH, and CASTNET sites when V_d of SO_2 is increased by 20%. It gives a slightly better model performance for NO_3^- at these sites, as a result of higher predicted NO_3^- concentrations by 2–4%. The reduction of SO_4^{2-} can increase NO_3^- because it frees up NH_3 to neutralize HNO_3; however it cannot improve the underpredictions of NH_4^+ as it causes a decrease in NH_4^+ concentrations at the SEARCH sites.

Cloud processes of SO_4^{2-} and gas–phase chemistry of SO_2. Cloud processes (e.g., dissolution of soluble gases, aqueous chemistry, scavenging, and wet deposition) have important impacts on SO_4^{2-} formation via the aqueous–phase SO_2 oxidations. Such an oxidation depends on the cloud liquid water content, pH, the concentrations of dissolved O_3 and H_2O_2, and cloud lifetime (Seinfeld and Pandis, 2006). As shown in Table 2, process analysis shows that several species have relatively high correlation coefficients with cloud processes, e.g., 0.3 for $PM_{2.5}$ at rural sites of SEARCH, 0.27 for SO_4^{2-} at IMPROVE, and 0.51 for NO_3^- at CASTNET. In this study, simulated cloud fractions (CF) are compared with the observations from the Automated Surface Observing System

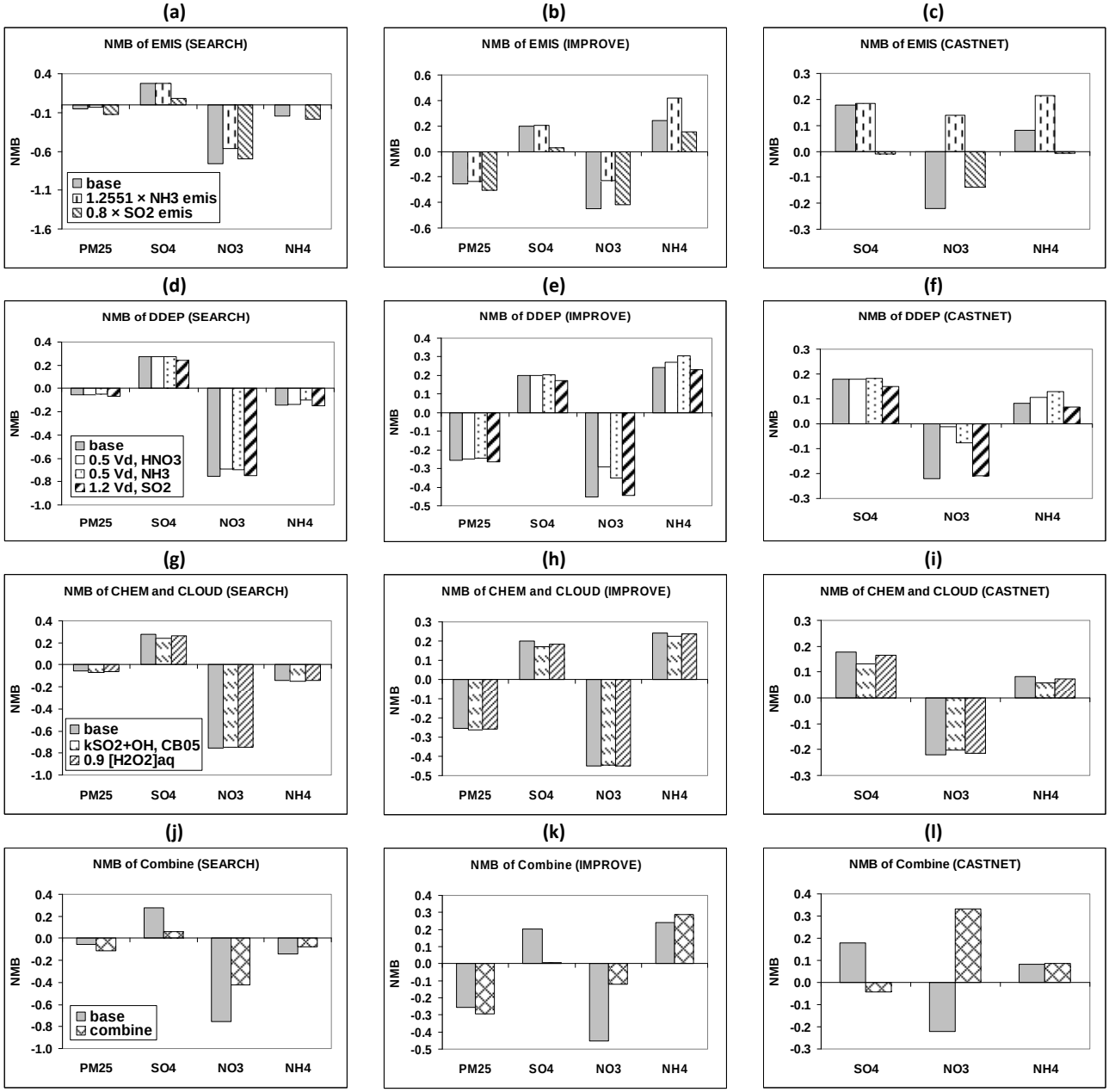

Figure 7. *Normalized mean biases (NMBs) of simulated NH_4^+, NO_3^-, SO_4^{2-}, and $PM_{2.5}$ (by CMAQ) for the baseline and various sensitivity simulations (**(a)-(c)**: adjusting NH_3 and SO_2 emissions; **(d)-(f)**: adjusting dry deposition velocity of HNO_3, NH_3, and SO_2; **(g)-(i)**: replacing the rate constant of reaction SO_2 and OH, and adjusting the dissolved concentrations of H_2O_2 in cloud droplets; **(j)-(l)**: multiple adjustments including 1.2551 × E_{NH3}, 0.8 × E_{SO2}, $K_{SO2+OH,\ CB05}$, and 0.84 × $V_{d,HNO3}$) at the IMPROVE, SEARCH, and CASTNET sites in June 14-28, 1999. Observed $PM_{2.5}$ concentrations are not available at the CASTNET sites.*

(ASOS) at 13 sites available in the southeastern U.S. ASOS contains the surface observations of hourly data for cloud height and coverage that can be converted to CF. The comparison shows that MM5 overestimates observed CFs by roughly 10% (simulated value of 0.403 vs. observed value of 0.376). Since adjusting CFs in the meteorological inputs may cause a self–inconsistency in the meteorological fields that are related and solved based on the continuity equation [Equation (1)], the dissolved concentrations of H_2O_2 in cloud droplets are adjusted using a dissolution efficiency factor of 0.9 that reflects the changes of CFs. As shown in Figures 7g–7i, the NMBs of SO_4^{2-} are slightly improved (decreasing by 2%) at all sites. However, the predicted mean SO_4^{2-} concentrations only decrease by 1% at all three sites compared with those from the baseline simulation. This indicates that a 10% reduction of dissolved H_2O_2 has negligible effects on SO_4^{2-} for this episode, due partly to the relatively scattered cloud conditions.

Another important formation of SO_4^{2-} is the gas–phase oxidation of SO_2 by OH. The rate constant of this reaction used in SAPRC99 is larger than that used in CB05 (Sarwar et al., 2008), especially under conditions with relatively low temperatures and high pressures. For example, when temperature is 288 K and pressure is 1013 Pa, the rate constant of SAPRC99 is 1.12 times of that of CB05. One sensitivity simulation is conducted using the rate constant in CB05, which can reduce SO_4^{2-} mass concentration by 3% and reduce its NMB from 20% to 17%, 24% to 20%, and 18% to 13%, respectively, at the IMPROVE, SEARCH, and CASTNET networks.

Among the above sensitivity simulations, adjusting NH_3 emissions and dry deposition velocity of HNO_3 lead to the most improvement to NO_3^- statistics. Adjusting SO_2 emissions and using the rate constant in CB05 for the SO_2(g) + OH reaction improve the SO_4^{2-} statistics the most. Finally, multiple adjustments are applied to one simulation to study the combined effects of those adjustments. The multiple adjustments are selected based on the individual sensitivity test that has the NMB improvement larger than 5%, including $1.2551 \times E_{NH3}$, $0.8 \times E_{SO2}$, $K_{SO2+OH, CB05}$, and $0.84 \times V_{d, HNO3}$. As compared with the value of 0.5 used in the individual sensitivity simulation, a larger adjustment factor of 0.84 is used here, which is derived based on the calculated $V_{d,HNO3}$ values from the CASTNET. The calculated $V_{d,HNO3}$ values in CASTNET were obtained by a dry deposition model, Multi Layer Model, using observed meteorological and canopy data from CASTNET. As shown in Figure 7, in this final simulation, SO_4^{2-} concentration is reduced by 16–19% and its NMBs are reduced from 20% to 1%, 24% to 3%, and 18% to 4%, respectively, at the IMPROVE, SEARCH, and CASTNET networks. NO_3^- concentration is increased by 74–127%. Its NMBs change from –45%, –75%, –22% to –12%, –42%, and 33% at the IMPROVE, SEARCH, and CASTNET sites, respectively. NH_4^+ concentration is increased by 1–8%. The NMB of NH_4^+ concentration is reduced from 32% to 27% at the SEARCH sites, but increased from 24% to 29% and from 8% to 9% at the IMPROVE and CASTNET sites. These statistics indicate an overall improvement of the model performance for SO_4^{2-} and NO_3^-, although the performance for $PM_{2.5}$ is slightly worse. Reducing model biases in individual PM compositions is meaningful, because a "seemly" good performance in $PM_{2.5}$ (e.g., in the baseline, compared with the sensitivity simulations with multiple adjustments) may result from a cancellation of positive and negative biases.

4. Summary

Process analysis is performed to understand governing atmospheric processes for key pollutants in order to reduce model biases. The O_3 chemistry regimes are examined by using P_{H2O2}/P_{HNO3} from IRRs during daytime and NO_y concentrations during afternoon as photochemical indicators. The results show a dominance of NO_X–sensitive chemistry over most U.S., and a dominance of VOC–sensitive chemistry in major cities in California, New England, and the Great Lakes and Ohio valley in the mid–west. The reductions in O_3 mixing ratios are not proportional to the reductions in NO_X or VOC emissions, indicating a non–linearity of the O_3 chemistry (e.g., the non–linearity caused by the inclusion of complex chemical reactions for O_3 formation and other non–linear atmospheric processes such as vertical mixing and wet removal). The IPRs show the relatively large net amount of exported O_X, O_3, AVOCs, and $PM_{2.5}$ from the PBL to the free troposphere, which can further affect the concentrations at the surface at downwind locations. Emissions are important sources for PM precursors such as SO_2, NO_X, and NH_3. Cloud processes contribute to the decrease of concentrations of SO_2, HNO_3, and NH_3. Aerosol processes contribute to a decrease in the concentrations of NH_3 but an increase in the concentrations of HNO_3. Horizontal transport and dry deposition are important removal processes for all PM precursors, particularly for HNO_3. Aerosol processes and emissions are the most important production processes for $PM_{2.5}$ and its secondary components. Horizontal and vertical transport and dry deposition contribute to their removal. Cloud processes can contribute to the production of $PM_{2.5}$ and SO_4^{2-} and the removal of NO_3^- and NH_4^+.

The IPRs correlation analysis is conducted for $PM_{2.5}$, SO_4^{2-}, NO_3^-, NH_4^+, and their precursors, HNO_3, NH_3, and SO_2. Horizontal transport is highly correlated with $PM_{2.5}$ biases at the STN sites. Vertical transport is correlated with SO_4^{2-} at rural sites from SEARCH, IMPROVE, and CASTNET. Emissions are slightly–to–moderately correlated to $PM_{2.5}$, SO_4^{2-}, and NO_3^- biases at some sites. Aerosol processes are correlated with the biases of $PM_{2.5}$, SO_4^{2-}, NO_3^-, and NH_4^+ at all sites from all networks, with larger model biases occurring for $PM_{2.5}$, NO_3^-, and NH_4^+ under dry or NH_3–rich conditions. Cloud processes are sometimes correlated with a few species such as $PM_{2.5}$ and NH_4^+ at the SEARCH rural sites, SO_4^{2-} at the IMPROVE sites, and NO_3^- at the CASTNET sites. Dry deposition is correlated with biases for all species, in particular SO_4^{2-} at all sites and NO_3^- at the IMPROVE and CASTNET sites. Guided from the PA results, several sensitivity simulations are performed to quantify the model response to major processes/reactions contributing to the model biases. The variables/processes examined include the dry deposition velocities of PM species (i.e., SO_4^{2-}) and precursors (i.e., HNO_3, NH_3, and SO_2), the emissions of PM precursors (i.e., NH_3 and SO_2), and the cloud processes and gas–phase chemistry of SO_4^{2-} formation. The decreased dry deposition velocities of HNO_3 and NH_3 can increase NO_3^- and NH_4^+ formation, therefore appreciably improving NO_3^- and NH_4^+ predictions when they both are underpredicted. Higher dry deposition velocity of SO_2 can increase NO_3^- and reduce NH_4^+. This can slightly improve model performance at the IMPROVE sites, but cannot improve the underpredictions of NH_4^+ at the SEARCH sites. Adjusting SO_4^{2-} dry deposition alone or together with SO_2 emission reduction has negligible impacts on $PM_{2.5}$ simulations especially for SO_4^{2-}. For this summer episode, when NH_3 emission is increased, both NO_3^- and NH_4^+ increase while SO_4^{2-} remains relatively constant. This indicates the sulfate–poor conditions at both the IMPROVE and SEARCH sites. Similarly to the cases with decreased dry deposition velocities of HNO_3 and NH_3, increased NH_3 emissions can appreciably improve the model performance when both NO_3^- and NH_4^+ are underpredicted. Reducing SO_2 emissions can reduce SO_4^{2-} by 15–16%, and reduce the absolute NMB by 79–94%. The sensitivity simulation with a dissolution efficiency factor of H_2O_2 shows that a 10% reduction of dissolved H_2O_2 cannot significantly affect SO_4^{2-} formation for this episode. Using the rate constant from CB05 for SO_2(g) + OH can reduce SO_4^{2-} by 3% and reduce the absolute NMB by 15–85%. Adjusting the most influential processes/factors (i.e., emissions of NH_3 and SO_2, dry deposition velocity of HNO_3, and gas–phase oxidation of SO_2 by OH) improves the model overall performance in terms of SO_4^{2-}, NO_3^-, and NH_4^+ (e.g., reducing NMBs from 24% to 3%, –75% to –42%, and 32% to 27% at the SEARCH sites, respectively). These

results suggest that improving treatments of these most influential processes/factors may improve model performance.

Acknowledgements and Disclaimer

This work was performed under the National Science Foundation Award No. Atm–0348819, and the Memorandum of Understanding between the U.S. Environmental Protection Agency (EPA) and the U.S. Department of Commerce's National Oceanic and Atmospheric Administration (NOAA) and under agreement number DW13921548. The authors thank Alice Gilliland and Steve Howard, U.S. NOAA/EPA, for providing the Fortran code for extracting data from CMAQ and the CASTNET, IMPROVE, and AIRS–AQS observational datasets, and Robert W. Pinder and Prakash Bhave, U.S. NOAA/EPA, for helpful discussions. Although this work was reviewed by EPA and approved for publication, it does not necessarily reflect their policies or views.

References

Arnold, J.R., Dennis, R.L., 2006. Testing CMAQ chemistry sensitivities in base case and emissions control runs at SEARCH and SOS99 surface sites in the southeastern US. *Atmospheric Environment* 40, 5027-5040.

Binkowski, F.S., Roselle, S.J., 2003. Models-3 community multiscale air quality (CMAQ) model aerosol component, 1. Model description. *Journal of Geophysical Research-Atmospheres* 108, art. no. 4183.

Byun, D.W., Ching, J.K.S., 1999. Science algorithms of the EPA Models-3 community multiscale air quality (CMAQ) modeling system, EPA/600/R-99/030, Office of Research and Development, U.S. Environmental Protection Agency, Washington, D.C.

Carter, W.P.L., 2000. Implementation of the SAPRC99 Chemical Mechanism into the Models-3 Framework, Report to the US Environmental Agency, http://www.engr.ucr.edu/~carter/pubs/s99mod3.pdf.

Finkelstein, P.L., Ellestad, T.G., Clarke, J.F., Meyers, T.P., Schwede, D.B., Hebert, E.O., Neal, J.A., 2000. Ozone and sulfur dioxide dry deposition to forests: observations and model evaluation. *Journal of Geophysical Research-Atmospheres* 105, 15365-15377.

Goebes, M.D., Strader, R., Davidson, C., 2003. An ammonia emission inventory for fertilizer application in the United States. *Atmospheric Environment 37*, 2539-2550.

Hogrefe, C., Lynn, B., Rosenzweig, C., Goldberg, R., Civerolo, K., Ku, J.Y., Rosenthal, J., Knowlton, K., Kinney, P.L., 2005. Utilizing CMAQ process analysis to understand the impacts of climate change on ozone and particulate matter. *The 4th Annual CMAS Models-3 User's Conference*, Sept 26-28, Chapel Hill, NC.

Jang, J.C.C., Jeffries, H.E., Tonnesen, S., 1995. Sensitivity of ozone to model grid resolution-II. Detailed process analysis for ozone chemistry. *Atmospheric Environment* 29, 3101-3114.

Jiang, G., Lamb, B., Westberg, H., 2003. Using back trajectories and process analysis to investigate photochemical ozone production in the Puget Sound region. *Atmospheric Environment* 37, 1489-1502.

Liu, P., Zhang, Y., 2011. Use of a process analysis tool for diagnostic study on fine particulate matter predictions in the U.S. Part I: model evaluation. *Atmospheric Pollution Research* 2, 49-60.

O'Neill, S.M., Lamb, B.K., 2005. Intercomparison of the community multiscale air quality model and CALGRID using process analysis. *Environmental Science and Technology* 39, 5742-5753.

Phillips, S.B., Arya, S.P., Aneja, V.P., 2004. Ammonia flux and dry deposition velocity from near-surface concentration gradient measurements over a grass surface in North Carolina. *Atmospheric Environment* 38, 3469-3480.

Sarwar, G., Luecken, D., Yarwood, G., Whitten, G.Z., Carter, W.P.L., 2008. Impact of an updated Carbon Bond Mechanism on predictions from the CMAQ modeling system: preliminary assessment, *Journal of Applied Meteorology and Climatology* 47, 3-14.

Seinfeld, J.H., Pandis, S.N., 2006. *Atmospheric Chemistry and Physics: From Air Pollution To Climate Change*, John Wiley and Sons, New York, NY.

Sillman, S., 1995. The use of NO_y, H_2O_2 and HNO_3 as indicators for Ozone-NO_x-hydrocarbon sensitivity in urban locations. *Journal of Geophysical Research-Atmospheres* 100, 14175-14188.

Sillman, S., He, D., 2002. Some theoretical results concerning O_3-NO_x-VOC chemistry and NO_x-VOC indicators. *Journal of Geophysical Research* 107, art. no. 4659.

Tonnesen, G.S., Dennis, R.L., 2000. Analysis of radical propagation efficiency to assess ozone sensitivity to hydrocarbons and NO_x. 1. Local indicators of instantaneous odd oxygen production sensitivity. *Journal of Geophysical Research* 105, 9213-9225.

Tonse, S.R., Brown, N.J., Harley, R.A., Jinc, L., 2008. A process-analysis based study of the ozone weekend effect. *Atmospheric Environment* 42, 7728-7736.

Wang, K., Zhang, Y., Jang, C., Phillips, S., Wang, B.B., 2009. Modeling study of intercontinental air pollution transport over the trans-Pacific region in 2001 using the community multiscale air quality modeling system. *Journal of Geophysical Research-Atmospheres* 114, art. no. D04307.

Wu, S.Y., Hu, J.L., Zhang, Y., Aneja, V.P., 2008. Modeling atmospheric transport and fate of ammonia in North Carolina - Part II: effect of ammonia emissions on fine particulate matter formation. *Atmospheric Environment* 42, 3437-3451.

Yu, S., Mathur, R., Schere, K., Kang, D., Pleim, J., Young, J., Tong, D., Pouliot, G., McKeen, S.A., Rao, S.T., 2008. Evaluation of real-time $PM_{2.5}$ forecasts and process analysis for $PM_{2.5}$ formation over the eastern United States using the Eta-CMAQ forecast model during the 2004 ICARTT study. *Journal of Geophysical Research-Atmospheres* 113, art. no. D06204.

Yu, S., Dennis, R.L., Bhave, P.V., Eder, B.K., 2004. Primary and secondary organic aerosols over the United States: estimates on the basis of observed organic carbon (OC) and elemental carbon (EC), and air quality modeled primary OC/EC ratios. *Atmospheric Environment* 38, 5257-5268.

Zhang, Y., 2008. Online coupled meteorology and chemistry models: history, current status, and outlook. *Atmospheric Chemistry and Physics* 8, 1833-1912.

Zhang, Y., Wen, X.Y., Jang, C.J., 2010a.Simulating chemistry–aerosol–cloud–radiation–climate feedbacks over the continental U.S. using the online-coupled Weather Research Forecasting Model with chemistry (WRF/Chem). *Atmospheric Environment* 44, 3568-3582.

Zhang, Y., Liu, P., Liu, X.H., Jacobson, M.Z., McMurry, P., Yu, F., Yu, S.C., Schere, K.L., 2010b. A comparative study of homogeneous nucleation parameterizations, Part II. Three dimensional model application and evaluation, *Journal of Geophysical Research-Atmospheres* 115, D20213.

Zhang, Y., Vijayaraghavan, K., Wen, X.Y., Snell, H.E., Jacobson, M.Z., 2009a. Probing into regional O_3 and particulate matter pollution in the United States, Part I. A 1-year CMAQ simulation and evaluation using surface and satellite data. *Journal of Geophysical Research-Atmospheres* 114, art. no. D22304.

Zhang, Y., Wen, X.Y., Wang, K., Vijayaraghavan, K., Jacobson, M.Z., 2009b. Probing into regional O_3 and PM pollution in the U.S., Part II. An examination of formation mechanisms through a process analysis technique and sensitivity study. *Journal of Geophysical Research-Atmospheres* 114, art. no. D22305.

Zhang, Y., Liu, P., Queen, A., Misenis, C., Pun, B., Seigneur, C., Wu, S.Y., 2006. A comprehensive performance evaluation of MM5-CMAQ for the Summer 1999 Southern Oxidants Study episode-Part II: gas and aerosol predictions. *Atmospheric Environment* 40, 4839-4855.

Zhang, Y., Vijayaraghavan, K., Seigneur, C., 2005. Evaluation of three probing techniques in a three-dimensional air quality model. *Journal of Geophysical Research-Atmospheres* 110, art. no. D02305.